Orange-Light-Induced Photochemistry Gated by pH and Confined Environments

Daniel Kodura, Leona L. Rodrigues, Sarah L. Walden, Anja S. Goldmann, Hendrik Frisch,* and Christopher Barner-Kowollik*

ABSTRACT: We introduce a new photochemically active compound, i.e., pyridinepyrene (PyPy), entailing a pH-active moiety that effects a significant halochromic shift into orange-light (λ = 590 nm) activatable photoreactivity while concomitantly exerting control over its reaction pathways. With blue light (λ = 450 nm) in neutral to basic pH, a [2 + 2] photocycloaddition can be triggered to form a cyclobutene ring in a reversible fashion. If the pH is decreased to acidic conditions, resulting in a halochromic absorption shift, photocycloaddition on the small-molecule level is blocked due to repulsive interactions and exclusive *trans-cis* isomerization is observed. Through implementation of PyPy into the confined environment of a single-chain nanoparticle (SCNP) design, one can overcome the repulsive forces and exploit the halochromic shift for orange light (λ = 590 nm)-induced cycloaddition and formation of macromolecular three-dimensional (3D) architectures.

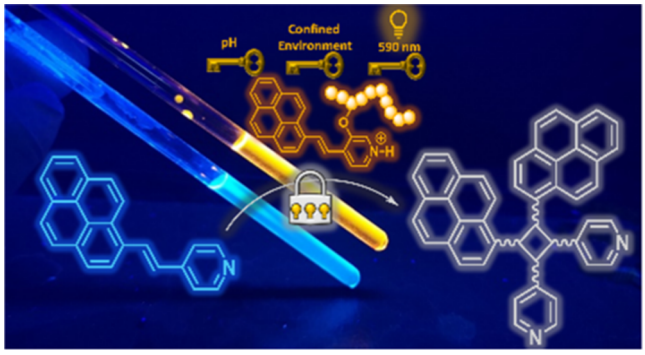

INTRODUCTION

Photochemistry, essentially enabling life on our planet,[1] has evolved into a powerful tool in modern synthesis, featuring versatility, efficiency, exquisite spatiotemporal control, and mild reaction conditions.[2−6] These factors make photochemical reactions applicable in various research areas such as three-dimensional (3D) printing,[7,8] catalysis,[9,10] and biology.[11,12] Shifting the activation wavelength of photochemical reactions well into the visible-light regime is one of the key challenges and main foci due to the considerable increase of penetration depth through matter.[13,14] Critically, shorter wavelength light, in particular UV light, is known for causing harm to biological environments,[15,16] but can also cause degradation of soft matter materials.[17]

To generate the desired red shift in light gated reactions, the highest occupied molecular orbital−lowest unoccupied molecular orbital (HOMO−LUMO) gap in a photoreactive molecule must be lowered. Approaches such as the expansion of the π-system through conjugation with extended aromatic systems like styrene,[18] pyrene,[19] and quinoxaline have been followed.[20] Introduction of electron-pushing substituents such as thiols[21,22] and amides[23] or electron-pulling groups such as nitro-groups[24] or halogens[25,26] can furthermore red shift the photoreactivity. In addition to adjusting the intrinsic molecular design, the group of Bach successfully established an alternative pathway of red-shifting activation energies. Through addition of an aluminum-based chiral Lewis acid, the activation wavelength of the intramolecular [2 + 2] photocycloaddition was shifted and performed in a regio- and diastereoselective manner.[27] Other Lewis[28] and Brønsted acids,[29] organocatalysts,[30] or simply protons[31] have been exploited in a similar fashion.

Importantly, photoreactivity also depends on the respective excited electronic transitions as well as the surrounding environment. If different excited states are populated through a switch of activation wavelength, a change in relaxation pathways can cause a change in the obtained photoproducts.[32] When attached to macromolecular structures such as polymer chains,[33] crystals,[34,35] or surfaces,[36,37] the reaction kinetics and λ-dependence of photoreactions can strongly differ from those in solution. The photocycloaddition of styrylpyrene, for example, can be triggered at significantly lower concentrations and at a previously reported inaccessible wavelength when contained in a polymer chain.[38,39] In contrast, the reversion triggered with UV light proceeds sluggishly due to an unfavorable photostationary state.[40]

Herein, we introduce the photochemistry of pyridinepyrene (**PyPy**), which can be controlled by pH and its macromolecular environment. Through the decoration of a pyridine moiety with a conjugated aromatic system containing a double bond accessible to [2 + 2] photocycloaddition, a halochromic system is established, opening highly defined reaction pathways. We investigate **PyPy**'s photochemistry at variable pH regimes (acidic, neutral, and basic) and within a wide wavelength regime (360−620 nm). Furthermore, we utilize the impact of a confined environment within a single polymer chain to induce a change in the reaction pathway, which enables orange-light-induced photocycloadditions.

RESULTS AND DISCUSSION

(*E*)-Pyridinepyrene ((***E***)-**PyPy**, Figure 1, violet) is pale yellow in solution (acetonitrile (ACN), c = 0.01 mM) and has its absorption maximum at λ = 373 nm with a strong blue fluorescence (λ_{max} = 458 nm).

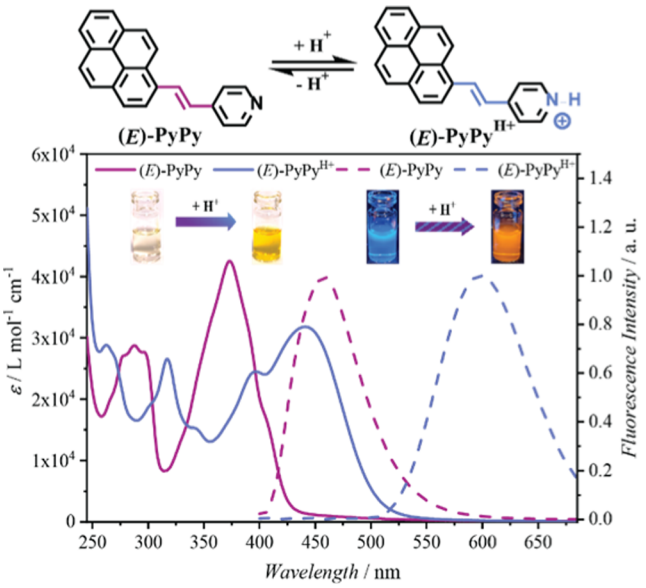

Figure 1. Top: Structure of (***E***)-**PyPy** (violet) and its protonated counterpart (***E***)-**PyPy**$^{H+}$ (blue). Bottom: UV−vis absorption (solid lines) and fluorescence spectra (λ = 350 nm, dashed lines) of the respective species. Pictures of the solutions in basic and protonated states at c = 0.01 mM as well as under a UV lamp (λ = 360 nm).

When protonated, (*E*)-pyridinepyrene^{H+} ((***E***)-**PyPy**$^{H+}$, blue) is formed, establishing an electron-deficient push−pull system, resulting in a significant red shift to a new maximum of λ = 440 nm. In addition, a strong yellow coloration of the solution occurs as well as an even stronger shift in its fluorescence (λ_{max} = 598 nm). Interestingly, the maximum molar absorptivity decreases by 25% going from (***E***)-**PyPy** (ε = 42 550 L mol^{-1} cm^{-1}) to (***E***)-**PyPy**$^{H+}$ (ε = 31 800 L mol^{-1} cm^{-1}) and an additional absorption band is observed in the protonated state (λ_{max} = 395 nm). Due to its halochromic characteristics, (***E***)-**PyPy** can undergo two reaction pathways when irradiated, controlled by pH. In neutral conditions, irradiation with blue LED (λ_{max} = 450 nm) induces cycloaddition, yielding different regioisomers of cyclobutane (**Dim-PyPy**, green) (Scheme 1). This process is reversible, as the cycloreversion can be activated when irradiated with a UV lamp (λ_{max} = 360 nm). However, if the pH is lowered and (***E***)-**PyPy**$^{H+}$ (blue) is formed, irradiation is unable to induce photocycloaddition, blocking this reaction pathway. Instead, photoisomerization occurs and (*Z*)-pyridinepyrene^{H+} ((***Z***)-**PyPy**$^{H+}$, orange) is generated. (***Z***)-**PyPy**$^{H+}$ is also locked in the protonated state and can only be converted to **Dim-PyPy** when deprotonated and irradiated with blue light.

Scheme 1. Overview of PyPy Reaction Pathways[a]

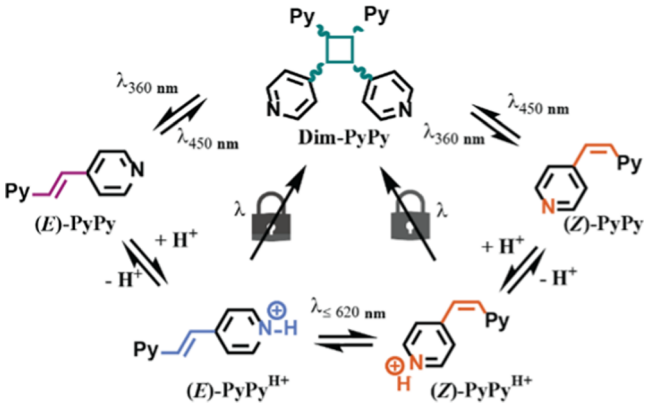

[a]Accessible and locked reaction pathways of pyridinepyrene (Py, pyrene).

We investigated the above-described reaction pathways in-depth using liquid chromatography-mass spectrometry (LC-MS) and ^{1}H NMR spectroscopy (Figure 2). Specifically, (***E***)-**PyPy** eluates at 8.6 min in the LC chromatogram (Figure 2) and is associated with a significant double-bond resonance at δ = 8.67 and 8.45 ppm. When irradiated in neutral conditions (c = 5 mM, ACN, deoxygenated) with a blue LED (λ_{max} = 450 nm, 10 h), five products are observed in the crude LC chromatogram (top row). The signals at retention times of 9.0 min (10% of cycloadducts), 9.5 min (37% of cycloadducts), and 10.3 min (53% of cycloadducts) belong to the different regioisomers of **Dim-PyPy** (refer to Figure S26 for all isomers and their geometry), yielding an overall conversion of more than 94%. Less than 2% (***Z***)-**PyPy** (8.1 min) and 4% of unconverted (***E***)-**PyPy** (8.6 min) are detected as minor side products. In the corresponding ^{1}H NMR spectra, the isolated isomer **Dim-PyPy-I** (9.5 min, *syn* head-to-tail) is associated with its characteristic cyclobutane resonances at δ = 5.93 and 5.12 ppm.[38] We determined the quantum yield for the cycloaddition as ϕ_{dimer} (%) = 0.19 ± 0.03 (refer to the Supporting Information section 3.9). In contrast, if (***E***)-**PyPy**$^{H+}$ (c = 5 mM, ACN, 10 eq. trifluoroacetic acid (TFA), deoxygenated) is irradiated with a green LED (λ_{max} = 525 nm, 10 h), (***Z***)-**PyPy**$^{H+}$ is the only product (yield 80%). This is apparent by the LC elution peak at 8.1 min as well as the *Z*-double-bond resonances in the ^{1}H NMR spectrum at δ = 7.68 and 6.95 ppm. Herby, the isomerization can also be conducted in a catalytic fashion with 5 mol% acid leading to the same isomeric pattern after irradiation (Figure S46). The quantum yield for the isomerization was determined as ϕ_{E-Z} (%) = 14 ± 2 (refer to the Supporting Information section 3.9). Remarkably, the UV−vis spectrum of the *Z*-isomer displays significant pyrene bands (Figure S1), an indication of the weaker conjugation within the push−pull system.

After neutralization, (***Z***)-**PyPy** was irradiated with a blue LED (λ_{max} = 450 nm) to promote dimer formation. As a result, a notably different pattern of the cyclobutane regioisomers is observed. **Dim-PyPy-II** (10.3 min, *syn* head-to-head, 60% of

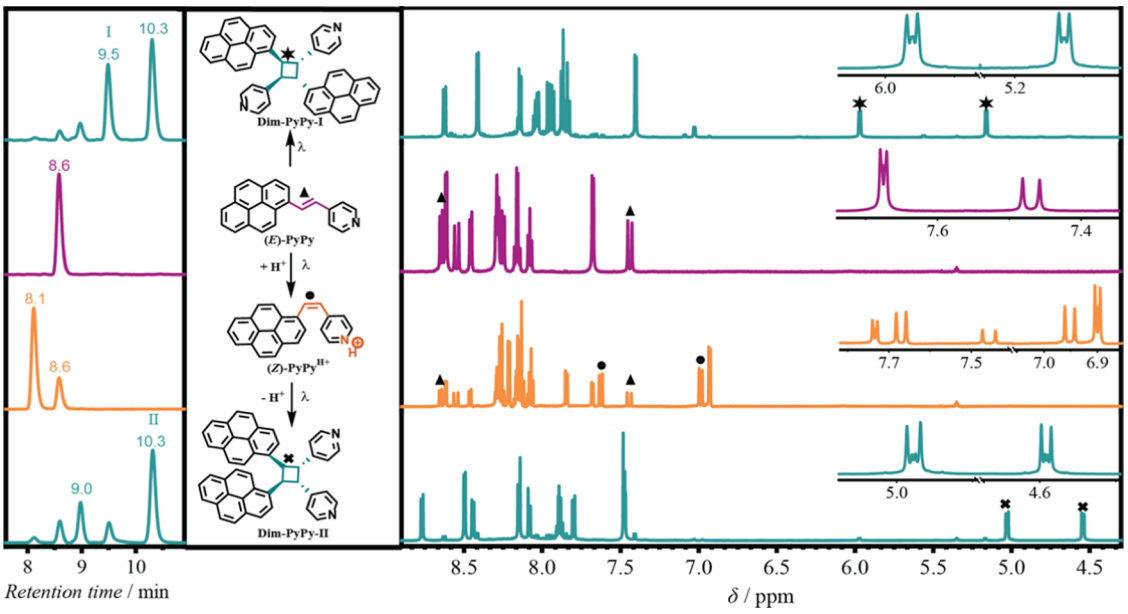

Figure 2. (left) LC chromatograms and (right) ^{1}H NMR spectra of the light-induced reaction pathways of pyridinepyrene (violet) (*E*)-**PyPy**. Irradiation with blue-light LED (λ_{max} = 450 nm) in neutral pH affords **Dim-PyPy-I** (green, LC of the crude reaction mixture, ^{1}H NMR of isolated **Dim-PyPy-I**). (*E*)-**PyPy** is irradiated with a green LED (λ_{max} = 525 nm) in acidic conditions to form (*Z*)-**PyPy^{H+}** (orange). (*Z*)-**PyPy^{H+}** is neutralized to (*Z*)-**PyPy** and irradiated with blue-light LED (λ_{max} = 450 nm) to form **Dim-PyPy-II** (green).

cycloadducts) is the main product, evident in the ^{1}H NMR spectrum (cyclobutane resonances at δ = 4.95 and 4.55 ppm). Additionally, the yield of **Dim-PyPy-III** (*anti* head-to-tail) increased noticeably to 25%, followed by a decrease of **Dim-PyPy-I** to merely 15%. This indicates that **Dim-PyPy-I** is exclusively accessible from the *trans* state. Thus, *via* specific pathways, we can manipulate the regioisomer ratios of the [2 + 2] photocycloaddition. To evidence reversibility of the system, a series of experiments was conducted to form the dimer and reverted it with UV light (λ_{max} = 360 nm) (Figures S3 and S41−43). To further investigate the photochemically induced isomerization process of (*E*)-**PyPy^{H+}** to (*Z*)-**PyPy^{H+}**, six solvents were screened for conversion to the *Z*-isomer. The isomerizations were conducted with solutions of c = 5 mM in the respective solvents, under deoxygenation and irradiation for a period of 16 h with a green LED (λ_{max} = 525 nm). The resulting yields of (*Z*)-**PyPy^{H+}** ranged from 54% (tetrahydrofuran (THF)) to 85% (dimethyl sulfoxide (DMSO)) (Table S1). These substantial differences are potentially useful for tuning of material properties.[41] The obtained isomers were tested for photochemical, mechanical, and thermal reversibility in acidic and neutral conditions. If heated (60 °C, 24 h) or sonicated (2 h), the isomer ratio did not change. Irradiation with UV light (λ = 350 nm) led to minor reversion in the protonated case (80/20 to 60/40 *Z*/*E*) and showed good reversibility in the deprotonated (*Z*)-PyPy (30/70 ratio *Z*/*E* after UV-light irradiation, Figure S45).

Due to the significant red shift in the protonated state, the lowest possible energy for activation of the isomerization in acetonitrile was explored. Specifically, a set of wavelengths ranging from λ = 550 to 620 nm was screened for reactivity, using a tunable laser setup. Remarkably, reactivity could be observed up to λ = 620 nm, corresponding to orange light (Figure S2). It is also evident that the reactivity decreases for wavelengths above λ = 560 nm.

To prove our hypothesis that the confined environment of a single polymer chain can overcome the restrictions hindering photocycloaddition in the protonated state, a **PyPy** containing monomer was designed (**M1**, Scheme S1) and incorporated into a pMMA copolymer *via* RAFT polymerization. The obtained polymer (**PyPyP**) has a molecular weight of 16 200 g mol^{-1} and a dispersity of D = 1.3. On average, 13 **PyPy** units are incorporated (Section S2), corresponding to 6−7 possible intramolecular cross-linking points. Initially, we focused on the established photocycloaddition in neutral conditions and investigated the folding behavior of this linear polymer into a single-chain nanoparticle (SCNP) with blue light (Figure 3A). Therefore, a solution of the polymer (c = 0.1 mg mL^{-1}) in tetrahydrofuran (THF) was prepared, deoxygenated, and irradiated with a blue LED (λ_{max} = 450 nm). The progress of the reaction was followed *via* UV−vis spectroscopy and size-exclusion chromatography (SEC) (Figure 3B/C). Rapidly (approx. 640 s), the reaction proceeds to completion, evidenced by the decrease in the main absorbance peak of the **PyPy** absorption at λ = 378 nm and the increase of the distinct pyrene bands with their maxima at λ = 330 and 350 nm. A clean reaction is observed, evidenced by the three isosbestic points of the photoreaction at λ = 288, 316, and 356 nm. The high local concentration and preorganization of the aromatic units within the polymer chain is likely responsible for the rapid reaction rate. In addition, the resulting intramolecular cross-linking of the polymer chains can be confirmed by the contraction of their hydrodynamic volume. As depicted in Figure 3C, with reaction time, the elution time in the SEC increases, caused by an increased number of intramolecular chain cross-links and the associated decrease of the hydrodynamic volume. Overall, the apparent molecular weight M_n decreased from 16 300 to 14 100 g mol^{-1}. In addition, diffusion-ordered NMR (DOSY, SI S3.2 and its appendix) measurements were conducted, demonstrating a decrease in the hydrodynamic radius from R_H = 2.98 ± 0.02 to 2.14 ± 0.04 nm (28% contraction).

Next, we investigated whether the halochromic shift of the protonated moiety can be exploited to initiate photo-

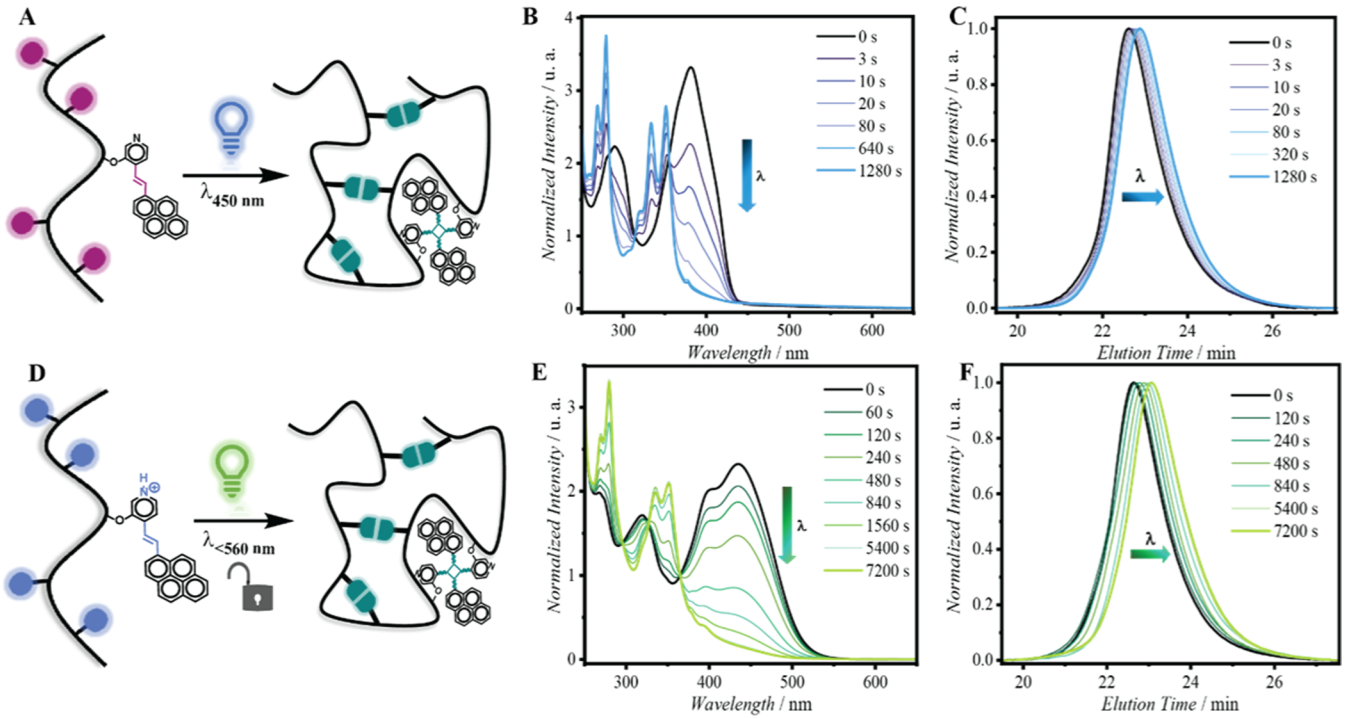

Figure 3. Folding of photoreactive chains into single-chain nanoparticles (SCNPs) *via* blue and green light. **A** Schematic drawing of photocycloaddition with blue light and neutral pH. **B** *In situ* UV−vis of **PyPyP** photocycloaddition in neutral conditions (THF, 0.1 mg mL ^{1}). **C** THF-SEC traces as a function of time mapping the folding process induced by a blue LED (λ_{max} = 450 nm) (UV trace at λ = 356 nm). **D** Schematic representation of the photocycloaddition of **PyPyP** in acidic conditions. **E** *In situ* UV−vis of **PyPyP** photocycloaddition in acidic conditions (THF, 0.1 mg·mL ^{1}). **F** THF-SEC traces as a function of time following the folding process induced by a green LED (λ_{max} = 525 nm) (UV trace at λ = 356 nm).

cycloaddition in the proximity of confined environments (Figure 3D). Thus far, in charged systems established by Whitten[42,43] and Yamada,[44] [2 + 2] photocycloaddition of charged moieties only occurred in the solid state or at very high concentrations above 1 M. As before, a solution of **PyPyP** (THF, c = 0.1 mg mL^{-1}) was acidified using 4 M HCl in dioxane (10 eq.), followed by deoxygenation. Subsequently, the solution was irradiated with a green LED (λ_{max} = 525 nm) and the reaction's progress was followed by *in situ* UV−vis and SEC (Figure 3E/F). The reaction proceeded very similarly to the neutral case with a decrease of the maximum absorption band at λ = 440 nm and the appearance of new pyrene bands. Critically, the reaction rate decreased considerably compared to the folding in neutral pH. Alternatively, the changed preorganization within the SCNP due to the present charge may cause the rate change. It is further evident that the shape of the resulting pyrene absorption band varies from the pyrene band observed during neutral folding. Yet, this can be overcome through neutralization of the solution, after which the product UV−vis appears as expected (Figure S4).

The change in hydrodynamic volume followed *via* SEC analysis displays a stepwise increase of elution time with proceeding reaction time. Overall, the apparent M_n decreased from 16 300 to 13 250 g mol^{-1}. DOSY analysis confirms this contraction, yielding a hydrodynamic radius of R_H = 2.17 ± 0.08 nm (27% contraction). The ^{1}H NMR spectra of the respective folded polymers (Figure S5) show cyclobutane resonances in the same regions (δ = 6.6−4.8 ppm), most likely corresponding to the different regioisomers. However, the ratio of the isomers varies in both polymers, indicating an impact of the pH on the selectivity for certain isomers. Whereas **Dim-PyPy-I** appears in the SCNP folded under neutral conditions (δ = 6.05−5.95 and 5.45−5.30 ppm), in the acidic folded SCNP, this isomer is significantly less favored. This could be explained by the foregoing **PyPy** isomerization followed by photocycloaddition due to the substantial decrease in the reaction rate, as previously demonstrated (Figure 2).

To assess whether the pH is truly responsible for the accessibility of the reaction with green light, the polymer was irradiated in neutral conditions in the same setup. Even after 2 h of irradiation, no change in the UV−vis or SEC was observed (Figure S6), proving the necessity of the protonation for halochromic photoreactivity. We subsequently examined whether light of a longer wavelength than green can induce photocycloaddition. Therefore, the irradiation of the protonated **PyPyP** was performed using an orange LED (λ_{max} = 590 nm). With a very slow reaction after four days of irradiation, a clear shift in the SEC traces as well as the appearance of pyrene bands in the UV−vis was observed, proving the reactivity at these high wavelengths (Figure S7).

CONCLUSIONS

In conclusion, we establish a new halochromic photoreactive molecule, pyridinepyrine (**PyPy**), with controllable reaction pathways depending on the pH and environment. **PyPy** can be reversibly dimerized in its unprotonated state with blue light/UV light. In contrast—when protonated—wavelengths up to λ = 620 nm induced isomerization ((*E*)-**PyPy** to (*Z*)-**PyPy**). We explored the impact of the double-bond stereochemistry on the resulting dimer regioisomers and were able to manipulate their ratios depending on the chosen pathways. Importantly, we transfer the photochemistry to a single-chain

nanoparticle and successfully formed a 3D architecture in both neutral and acidic conditions, illustrating environmental confinement effects allowing the photoreaction to proceed under exceptionally mild wavelengths.

■ ASSOCIATED CONTENT

● Supporting Information

The Supporting Information is available free of charge at https://pubs.acs.org/doi/10.1021/jacs.2c00156.

Materials, instrumentation, synthetic procedures, supporting spectroscopic data (PDF)

■ AUTHOR INFORMATION

Corresponding Authors

Hendrik Frisch − *School of Chemistry and Physics, Queensland University of Technology (OUT), Brisbane, QLD 4000, Australia; Centre for Materials Science, Queensland University of Technology, Brisbane, QLD 4000, Australia;* orcid.org/0000-0001-8490-5082; Email: h.frisch@qut.edu.au

Christopher Barner-Kowollik − *School of Chemistry and Physics, Queensland University of Technology (OUT), Brisbane, QLD 4000, Australia; Centre for Materials Science, Queensland University of Technology, Brisbane, QLD 4000, Australia; Institute of Nanotechnology, Karlsruhe Institute of Technology (KIT), 76344 Eggenstein-Leopoldshafen, Germany;* orcid.org/0000-0002-6745-0570; Email: christopher.barnerkowollik@qut.edu.au

Authors

Daniel Kodura − *School of Chemistry and Physics, Queensland University of Technology (OUT), Brisbane, QLD 4000, Australia; Centre for Materials Science, Queensland University of Technology, Brisbane, QLD 4000, Australia*

Leona L. Rodrigues − *School of Chemistry and Physics, Queensland University of Technology (OUT), Brisbane, QLD 4000, Australia; Centre for Materials Science, Queensland University of Technology, Brisbane, QLD 4000, Australia*

Sarah L. Walden − *School of Chemistry and Physics, Queensland University of Technology (OUT), Brisbane, QLD 4000, Australia; Centre for Materials Science, Queensland University of Technology, Brisbane, QLD 4000, Australia;* orcid.org/0000-0002-7625-4010

Anja S. Goldmann − *School of Chemistry and Physics, Queensland University of Technology (OUT), Brisbane, QLD 4000, Australia; Centre for Materials Science, Queensland University of Technology, Brisbane, QLD 4000, Australia*

Complete contact information is available at: https://pubs.acs.org/10.1021/jacs.2c00156

Author Contributions

The manuscript was written through contributions of all authors. All authors have given approval to the final version of the manuscript.

Notes

The authors declare no competing financial interest.

■ ACKNOWLEDGMENTS

A.S.G., H.F., and C.B.-K. acknowledge continued support from the Queensland University of Technology (QUT) and the Centre for Materials Science. H.F. acknowledges support by the Australian Research Council (ARC) in the form of a DECRA Fellowship and C.B.-K. in the form of an ARC Laureate Fellowship enabling his photochemical research program. C.B.-K. additionally acknowledges funding in the context of an ARC Discovery Grant focused on red-shifting photochemical reactions. Some of the data reported in this study were obtained at the Central Analytical Research Facility (CARF) operated by QUT's Research Portfolio.

■ REFERENCES

(1) Green, N. J.; Xu, J.; Sutherland, J. D. Illuminating Life's Origins: UV Photochemistry in Abiotic Synthesis of Biomolecules. *J. Am. Chem. Soc.* **2021**, *143*, 7219−7236.

(2) Buglioni, L.; Raymenants, F.; Slattery, A.; Zondag, S. D. A.; Noël, T. Technological Innovations in Photochemistry for Organic Synthesis: Flow Chemistry, High-Throughput Experimentation, Scale-up, and Photoelectrochemistry. *Chem. Rev.* **2022**, *122*, 2752−2906.

(3) Liu, J.; Lu, L.; Wood, D.; Lin, S. New Redox Strategies in Organic Synthesis by Means of Electrochemistry and Photochemistry. *ACS Cent. Sci.* **2020**, *6*, 1317−1340.

(4) Dutta, S.; Rühle, J.; Schikora, M.; Deussner-Helfmann, N.; Heilemann, M.; Zatsepin, T.; Duchstein, P.; Zahn, D.; Knör, G.; Mokhir, A. Red light-triggered photoreduction on a nucleic acid template. *Chem. Commun.* **2020**, *56*, 10026−10029.

(5) Beeler, A. B. Introduction: Photochemistry in Organic Synthesis. *Chem. Rev.* **2016**, *116*, 9629−9630.

(6) Irshadeen, I. M.; Walden, S. L.; Wegener, M.; Truong, V. X.; Frisch, H.; Blinco, J. P.; Barner-Kowollik, C. Action Plots in Action: In-Depth Insights into Photochemical Reactivity. *J. Am. Chem. Soc.* **2021**, *143*, 21113−21126.

(7) Wei, H.; Lei, M.; Zhang, P.; Leng, J.; Zheng, Z.; Yu, Y. Orthogonal photochemistry-assisted printing of 3D tough and stretchable conductive hydrogels. *Nat. Commun.* **2021**, *12*, No. 2082.

(8) Kuang, X.; Wu, J.; Chen, K.; Zhao, Z.; Ding, Z.; Hu, F.; Fang, D.; Qi, H. J. Grayscale digital light processing 3D printing for highly functionally graded materials. *Sci. Adv.* **2019**, *5*, No. eaav5790.

(9) Chen, G.; Waterhouse, G. I. N.; Shi, R.; Zhao, J.; Li, Z.; Wu, L.-Z.; Tung, C.-H.; Zhang, T. From Solar Energy to Fuels: Recent Advances in Light-Driven C1 Chemistry. *Angew. Chem., Int. Ed.* **2019**, *58*, 17528−17551.

(10) Rikken, G. L. J. A.; Raupach, E. Enantioselective magnetochiral photochemistry. *Nature* **2000**, *405*, 932−935.

(11) Zhang, M.; Li, K.; Bai, J.; Velema, W. A.; Yu, C.; van Damme, R.; Lee, W. H.; Corpuz, M. L.; Chen, J.-F.; Lu, Z. Optimized photochemistry enables efficient analysis of dynamic RNA structuromes and interactomes in genetic and infectious diseases. *Nat. Commun.* **2021**, *12*, No. 2344.

(12) Kowalik, L.; Chen, J. K. Illuminating developmental biology through photochemistry. *Nat. Chem. Biol.* **2017**, *13*, 587−598.

(13) Jia, S.; Sletten, E. M. Spatiotemporal Control of Biology: Synthetic Photochemistry Toolbox with Far-Red and Near-Infrared Light. *ACS Chem. Biol.* **2021**, DOI: 10.1021/acschembio.1c00518.

(14) Ash, C.; Dubec, M.; Donne, K.; Bashford, T. Effect of wavelength and beam width on penetration in light-tissue interaction using computational methods. *Lasers Med. Sci.* **2017**, *32*, 1909−1918.

(15) Marie, M.; Bigot, K.; Angebault, C.; Barrau, C.; Gondouin, P.; Pagan, D.; Fouquet, S.; Villette, T.; Sahel, J.-A.; Lenaers, G.; Picaud, S. Light action spectrum on oxidative stress and mitochondrial damage in A2E-loaded retinal pigment epithelium cells. *Cell Death Discovery* **2018**, *9*, No. 287.

(16) Nakazawa, H.; English, D.; Randell, P. L.; Nakazawa, K.; Martel, N.; Armstrong, B. K.; Yamasaki, H. UV and skin cancer:

specific p53 gene mutation in normal skin as a biologically relevant exposure measurement. *Proc. Natl. Acad. Sci. U.S.A.* **1994**, *91*, 360−364.
(17) Zayat, M.; Garcia-Parejo, P.; Levy, D. Preventing UV-light damage of light sensitive materials using a highly protective UV-absorbing coating. *Chem. Soc. Rev.* **2007**, *36*, 1270−1281.
(18) Peterson, J. A.; Wijesooriya, C.; Gehrmann, E. J.; Mahoney, K. M.; Goswami, P. P.; Albright, T. R.; Syed, A.; Dutton, A. S.; Smith, E. A.; Winter, A. H. Family of BODIPY Photocages Cleaved by Single Photons of Visible/Near-Infrared Light. *J. Am. Chem. Soc.* **2018**, *140*, 7343−7346.
(19) Doi, T.; Kawai, H.; Murayama, K.; Kashida, H.; Asanuma, H. Visible-Light-Triggered Cross-Linking of DNA Duplexes by Reversible [2+2] Photocycloaddition of Styrylpyrene. *Chem. - Eur. J.* **2016**, *22*, 10533−10538.
(20) Kalayci, K.; Frisch, H.; Truong, V. X.; Barner-Kowollik, C. Green light triggered [2+2] cycloaddition of halochromic styrylquinoxaline—controlling photoreactivity by pH. *Nat. Commun.* **2020**, *11*, No. 4193.
(21) Feist, F.; Menzel, J. P.; Weil, T.; Blinco, J. P.; Barner-Kowollik, C. Visible Light-Induced Ligation via o-Quinodimethane Thioethers. *J. Am. Chem. Soc.* **2018**, *140*, 11848−11854.
(22) Ludwanowski, S.; Hoenders, D.; Kalayci, K.; Frisch, H.; Barner-Kowollik, C.; Walther, A. Modular functionalization and hydrogel formation via red-shifted and self-reporting [2+2] cycloadditions. *Chem. Comm.* **2021**, *57*, 805−808.
(23) Mourot, A.; Kienzler, M. A.; Banghart, M. R.; Fehrentz, T.; Huber, F. M. E.; Stein, M.; Kramer, R. H.; Trauner, D. Tuning Photochromic Ion Channel Blockers. *ACS Chem. Neurosci.* **2011**, *2*, 536−543.
(24) Goulet-Hanssens, A.; Corkery, T. C.; Priimagi, A.; Barrett, C. J. Effect of head group size on the photoswitching applications of azobenzene Disperse Red 1 analogues. *J. Mater. Chem.* **2014**, *2*, 7505−7512.
(25) Bléger, D.; Schwarz, J.; Brouwer, A. M.; Hecht, S. o-Fluoroazobenzenes as Readily Synthesized Photoswitches Offering Nearly Quantitative Two-Way Isomerization with Visible Light. *J. Am. Chem. Soc.* **2012**, *134*, 20597−20600.
(26) Konrad, D. B.; Savasci, G.; Allmendinger, L.; Trauner, D.; Ochsenfeld, C.; Ali, A. M. Computational Design and Synthesis of a Deeply Red-Shifted and Bistable Azobenzene. *J. Am. Chem. Soc.* **2020**, *142*, 6538−6547.
(27) Brimioulle, R.; Bach, T. Enantioselective Lewis Acid Catalysis of Intramolecular Enone [2+2] Photocycloaddition Reactions. *Science* **2013**, *342*, 840−843.
(28) Brimioulle, R.; Guo, H.; Bach, T. Enantioselective Intramolecular [2+2] Photocycloaddition Reactions of 4-Substituted Coumarins Catalyzed by a Chiral Lewis Acid. *Chem. - Eur. J.* **2012**, *18*, 7552−7560.
(29) Pecho, F.; Sempere, Y.; Gramüller, J.; Hörmann, F. M.; Gschwind, R. M.; Bach, T. Enantioselective [2 + 2] Photocycloaddition via Iminium Ions: Catalysis by a Sensitizing Chiral Brønsted Acid. *J. Am. Chem. Soc.* **2021**, *143*, 9350−9354.
(30) Müller, C.; Bauer, A.; Bach, T. Light-Driven Enantioselective Organocatalysis. *Angew. Chem., Int. Ed.* **2009**, *48*, 6640−6642.
(31) Yamada, S.; Nojiri, Y. [2 + 2] Photodimerization of Naphthylvinylpyridines through Cation-π Interactions in Acidic Solution. *Molecules* **2017**, *22*, 491.
(32) Protti, S.; Ravelli, D.; Fagnoni, M. Wavelength dependence and wavelength selectivity in photochemical reactions. *Photochem. Photobiol. Sci.* **2019**, *18*, 2094−2101.
(33) Frisch, H.; Kodura, D.; Bloesser, F. R.; Michalek, L.; Barner-Kowollik, C. Wavelength-Selective Folding of Single Polymer Chains with Different Colors of Visible Light. *Macromol. Rapid Commun.* **2020**, *41*, No. 1900414.
(34) Bhogala, B. R.; Captain, B.; Parthasarathy, A.; Ramamurthy, V. Thiourea as a Template for Photodimerization of Azastilbenes. *J. Am. Chem. Soc.* **2010**, *132*, 13434−13442.
(35) Friščić, T.; Elacqua, E.; Dutta, S.; Oburn, S. M.; MacGillivray, L. R. Total Syntheses Supramolecular Style: Solid-State Construction of [2.2]Cyclophanes with Modular Control of Stereochemistry. *Cryst. Growth Des.* **2020**, *20*, 2584−2589.
(36) Zdobinsky, T.; Sankar Maiti, P.; Klajn, R. Support Curvature and Conformational Freedom Control Chemical Reactivity of Immobilized Species. *J. Am. Chem. Soc.* **2014**, *136*, 2711−2714.
(37) Kehrloesser, D.; Baumann, R.-P.; Kim, H.-C.; Hampp, N. Photochemistry of Coumarin-Functionalized SiO2 Nanoparticles. *Langmuir* **2011**, *27*, 4149−4155.
(38) Marschner, D. E.; Frisch, H.; Offenloch, J. T.; Tuten, B. T.; Becer, C. R.; Walther, A.; Goldmann, A. S.; Tzvetkova, P.; Barner-Kowollik, C. Visible Light [2 + 2] Cycloadditions for Reversible Polymer Ligation. *Macromolecules* **2018**, *51*, 3802−3807.
(39) Frisch, H.; Menzel, J. P.; Bloesser, F. R.; Marschner, D. E.; Mundsinger, K.; Barner-Kowollik, C. Photochemistry in Confined Environments for Single-Chain Nanoparticle Design. *J. Am. Chem. Soc.* **2018**, *140*, 9551−9557.
(40) Liu, M.; Wenzel, W.; Frisch, H. Photocycloreversions within single polymer chains. *Polym. Chem.* **2020**, *11*, 6616−6623.
(41) Goulet-Hanssens, A.; Eisenreich, F.; Hecht, S. Enlightening Materials with Photoswitches. *Adv. Mater.* **2020**, *32*, No. 1905966.
(42) Quina, F. H.; Whitten, D. G. Medium effects on photochemical reactions. Photochemistry of surfactant alkyl-4-stilbazole salts in solution, in the solid state, and in monolayer assemblies. *J. Am. Chem. Soc.* **1975**, *97*, 1602−1603.
(43) Whitten, D. G.; Russell, J. C.; Schmehl, R. H. Photochemical reactions in organized assemblies: environmental effects on reactions occurring in micelles, vesicles, films and mutilayer assemblies and at interfaces. *Tetrahedron* **1982**, *38*, 2455−2487.
(44) Yamada, S.; Uematsu, N.; Yamashita, K. Role of Cation−π Interactions in the Photodimerization of trans-4-Styrylpyridines. *J. Am. Chem. Soc.* **2007**, *129*, 12100−12101.